SUMMARY

This map provides regional information for assessing the potential for high-temperature (>150°C) geothermal systems in the Great Basin-those most likely to be capable of producing electrical energy. Three different maps have been overlain to produce the overall map shown here. The three component maps are:

1) A favorability map for high-temperature (>150°C) amagmatic-type geothermal systems. As discussed by Koenig and McNitt (1983) and Wisian and others (1999), amagmatic or extensional-type geothermal systems are those that do not obtain their heat from upper crustal magmas or cooling intrusions and instead are believed to owe their existence to active extensional or transtensional tectonics, Quaternary faults, and high regional heat flow. Deep circulation of meteoric waters along active faults in areas of high temperature gradient allows groundwater to be heated to relatively high temperatures at relatively shallow depths (1-3 km). The background colors, superimposed on shaded topography, provide a ranking of the favorability for amagmatic-type geothermal systems.

2) A favorability map for high-temperature (>150°C) magmatically heated geothermal systems, i.e., those believed to obtain their heat from upper crustal magmas or cooling intrusions. The favorability of magmatically heated geothermal systems is not color-ranked here, but can be assessed qualitatively based on the occurrence of Quaternary silicic volcanic vents (see red stars on map).

3) A geothermal information map. Superimposed on the color-scaled geothermal ranking are temperature gradient and heat flow measurements from wells (Southern Methodist University database), Quaternary faults (U. S. Geological Survey [USGS] compiled database), thermal springs and wells with geothermometer temperature estimates (Geo-Heat Center compiled database, Boyd, 2002), and geothermal power plants.

This map may be updated when more data become available or if alternate methods of GIS analysis are used. The map and the digital data layers used to build it are available on-line at http://www.unr.edu/geothermal/

AMAGMATIC GEOTHERMAL SYSTEMS — COLOR-SCALED FAVORABILITY RANKING

Warmer background colors on the map represent progressively greater favorability for high-temperature (>150°C) amagmatic-type geothermal systems. This classification is relative to the Great Basin only. Because the Great Basin has a relatively high geothermal favorability compared to most other areas of the United States (Blackwell and Richards, 2004), areas of low ranking (blue) on the Great Basin map might be considered favorable in the context of the entire continental United States, and could be favorable for lower-temperature (<150°C) geothermal applications. The number of colors displayed on this map has been maximized to highlight local changes in favorability.

The favorability rankings on the map are based on a "posterior probability" prediction: the warmer the color, the higher the probability of occurrence of a high-temperature geothermal system. The posterior probability was statistically derived using several input "evidence" maps, which include (1) a map of combined horizontal gravity gradient and horizontal topographic gradient, (2) a map combining crustal dilation as measured by Global Positioning System (GPS) stations and extension calculated from slip rates along Quaternary faults, (3) the temperature gradient in the upper crust, and (4) a map of the number, magnitude, and distance to historical earthquakes. Because host rock lithologies at 1-3 km depths (the assumed range in production depth) are either unknown or are poorly constrained in many areas, host rock compositions were not directly input into this model, and consequently the favorability ranking is independent of this parameter.

All known geothermal systems in the Great Basin (51 in total) that are either producing electrical power or have geothermometer temperatures >150°C were used as "training sites" to assess the degree of correlation between the input evidence maps and geothermal activity. Weights-of-evidence statistical analysis (Bonham-Carter and others, 1989; Bonham-Carter, 1996; Raines and others, 2000) was used to convert each real-number-based digital evidence map into a statistically significant number of ranked classes, based on the observed association with the geothermal systems. The gravity/topographic gradient evidence map was converted into five statistically significant classes of increasing gradient, while the crustal dilation. The temperature gradient evidence maps were each converted into maps with three levels of classification, and the earthquake evidence map was converted into a binary class map (favorable vs. unfavorable based on the distance from the nearest historical earthquake). These were used to combine the individual input evidence maps into an output predictive map, as described in the section on the occurrence of geothermal system. The color ranking on the map is proportional to the log-transformed logistic regression posterior probability. Logistic regression was chosen from many forms of regression because the dependent variable is a dichotomy (presence or absence of a geothermal system) and because the use of logistic regression does not require conditional independence between the independent variables (evidence layers) in regards to the dependent variable (Agterberg and others, 1993). More details on the application of weights-of-evidence and logistic regression analysis for modeling geothermal favorability are provided by Coolbaugh (2003) and Coolbaugh and others (2002).

The posterior probability scale is subdivided into several broad qualitative ranks of favorability, each of which spans roughly three standard deviations of error of the estimate. The lowest rank is "Permissive." Because all portions of the Great Basin are tectonically active to some degree and have an elevated potential for hosting a geothermal system compared to most of North America, all portions of the Great Basin are considered at least permissive for high-temperature geothermal activity. Higher favorability ranks have better combinations of the evidence indicative of geothermal activity. The "Most Favorable" rank is characterized by high gravity/topographic gradients, high strain rates, and high temperature gradients, whereas the "Permissive" rank encompasses areas with lower temperature gradients, strain rates, and gravity/topographic gradients. Where map colors correspond to the "Prior Probability" in the key, the evidential layers have served to neither enhance nor detract from the geothermal potential, with the net effect that these areas have average geothermal potential relative to the Great Basin.

TREATMENT OF REGIONAL AQUIFERS:
Most known high-temperature geothermal systems (>150°C) in the Great Basin occur outside regional groundwater aquifers (fig. 5), including the Snake River Plain and Northwest Basalt aquifers in the northern Great Basin (USGS Principal Aquifers of the 48 Conterminous United States, Hawaii, Puerto Rico, and the U.S. Virgin Islands, http://mapsonline.cr.usgs.gov/data/pa.html) and the Carbonate aquifer in eastern Nevada and western Utah (Prudic and others, 1996). It is hypothesized that lateral groundwater flow could be capturing and disarming rising thermal fluids, suppressing the occurrence of hot springs and reducing near-surface heat flow, thereby rendering these areas less completely explored than elsewhere in the Great Basin. To minimize potential bias with regard to aquifers in the favorability map, the geological and geophysical maps were preselected for their ability to model geothermal potential independent of the presence of these aquifers (at least at economic depths of <3 km). As a first step, weights-of-evidence and logistic regression model weights for each evidence map were calculated only in the non-aquifer areas (fig. 5). Those weights were then used to extrapolate geothermal favorability beneath areas having overlying regional aquifers. The logistic regression model accurately predicted 33 known geothermal training sites in non-aquifer regions, but predicted 23 training sites in the aquifer areas, whereas only 18 are known. This difference is statistically significant and suggests that the regional aquifers may be somewhat under-explored relative to other areas.

INPUT MAPS (MODEL LAYERS):
No geological/geophysical maps were combined into four evidence layers to model geothermal favorability. A description of each of these four layers follows:

1) Combined Gravity/Topographic Gradient Map – Figure 1 (Gary Oppliger): Geothermal activity is closely associated with young faults (Koenig and McNitt, 1983; Wisian and others, 1999; Bowen, 1989, p. 70), but not all faults in the Great Basin have been mapped, and the precise locations of many faults in the Great Basin are otherwise obscured by Quaternary sediments and playa deposits. The most active normal faults are likely to have relatively large vertical displacements, and in many cases this displacement will have placed relatively dense basement rocks against relatively light unconsolidated sediments. As a proxy for measuring the effective vertical displacement on late Tertiary and Quaternary faults in the Great Basin, a residual gravity map was combined with a topographic digital elevation model (DEM), and then the total surface slope (horizontal gradient) was calculated. The residual gravity map was further reduced by removing bedrock-only regional gravity trends to produce a basins-only gravity anomaly map. This gravity map was converted to an approximate equivalent amount of subsurface basement relief using 60 mGal (equivalent to a density contrast of 0.4 g/cm^3), and then added to the 1-km DEM. The combined bedrock surface slope was then calculated by computing the total horizontal gradient for each 1-km cell. Areas on this map with steep gradients correlate well with high temperature geothermal activity.

2) Crustal Dilation Map – Figure 2 (Corné Kreemer, Geoff Blewitt): Areas in the Great Basin with relatively high rates of crustal dilation, as mapped using GPS velocity measurements, have been shown by Blewitt and others (2002, 2003) to correlate with high-temperature geothermal activity, presumably because high dilation rates correspond to areas of active normal faulting which facilitate deep circulation of meteoric waters. Similarly, high slip rates on Quaternary normal faults, estimated from trench and geomorphological studies, also help delineate elevated geothermal potential. For this map, crustal dilation rates derived from GPS velocity measurements (intersesmic strain) were added to dilation rates calculated from Quaternary fault slip-rate data (long-term seismic strain) to produce a more geographically complete map of crustal dilation in the Great Basin. The geodetic strain rates were based on 476 GPS velocity measurements from stations located throughout and just outside the Great Basin. These velocities were compiled from multiple networks, including BARGEN (Bennett and others, 1998), USGS campaigns (e.g., Svarc and others, 2002; Hammond and Thatcher, 2004), and other groups. Velocities affected by known magmatic/volcanic activity were excluded. A USGS Quaternary Fault and Fold Database (Machette and others, 2003; http://qfaults.cr.usgs.gov/), was updated with slip-rate estimates compiled in 1996 and 2002 (http://pubs.usgs.gov/of/1996/of96-002/htmlfile/of2002.html). Slip-rate parameters were converted to long-term strain-rate tensors, from which dilation was calculated for every .20-km square grid cell in the Great Basin. The methodology used to obtain strain-rate models from GPS velocities and fault parameters (Haines and Holt, 1993; Holt and others, 2000; and Kreemer and others, 2003) is a rapidly evolving science. Significant improvements are expected in the future as the digital databases expand and measurement accuracies improve. Future work should help resolve apparent disparities between short-term and long-term fault slip-rates and clarify the distribution of slip along multiple sub-parallel fault segments. The network of GPS stations is rapidly expanding to provide better representation over a larger portion of the Great Basin.

3) Temperature Gradient Map – Figure 3 (David Blackwell, Maria Richards): Geothermal systems correlate with regions of high heat flow (Sass and others, 1971; Wisian and others, 1999) High heat flow brings more thermal energy close to the Earth's surface where it can heat circulating meteoric fluids. In this study, it was hypothesized that high temperature gradients may also be good predictors of geothermal potential, based on the argument that, the depths necessary to reach economic temperatures will be shallower when the temperature gradient is high, and fractures can more easily stay open at these relatively shallow depths. Weights-of-evidence analysis showed that high-temperature (>150°C) geothermal systems in the Great Basin correlate somewhat better with temperature gradient than with heat flow, and consequently temperature gradient, rather than heat flow, was chosen as an evidence layer in the model. A shallow crustal (0-1 km) temperature gradient map was generated using the SMU geothermal well database, which includes wells compiled by SMU (http://www.smu.edu/geothermal/), the USGS (Sass and others, 1999; http://pubs.usgs.gov/of/1999/of99-425/webmaps/home.html; http://pubs.usgs.gov/of/2005/1237/), and other sources. These combined databases contain more than 4,000 wells ranging to 5 km in depth. Temperature gradients were derived in a multi-step process beginning with calculation of heat flow at individual wells, interpolation of heat flow between wells to produce a heat flow map (e.g., Blackwell and Richards, 2004), and then conversion of the heat flow map to a temperature gradient map using thermal conductivities assigned for grouped geological formations. Improvements in the spatial resolution of the gradient map were obtained by assigning separate thermal conductivities to graben-filled Quaternary sediments, basement rocks in horst blocks, and regions of late Tertiary and Quaternary volcanic rocks. Purposely excluded from these calculations were wells with heat flows >120 mW/m^2 and wells with isothermal or negative gradients. This was done so the predicted temperature gradients would not be overly influenced by geothermal systems.

4) Seismicity Map – Figure 4 (Aasha Pancha): Earthquakes reveal areas of active faulting where pathways for deeply circulating hydrothermal fluids could be present. Weights-of-evidence analysis confirmed that zones of higher seismicity broadly correlate with geothermal activity. The seismicity map (fig. 4) was generated by summing all historical earthquake magnitudes within a 40-km radius of each grid cell. The distance from the epicenter to the center of each cell inversely weighted individual earthquake magnitudes. To avoid bias in the detection of earthquakes, earthquakes were not included in the seismicity calculation unless they were strong enough to be detected regardless of their location relative to seismograph stations. Earthquakes with a magnitude of >4.8 were considered to meet this criterion regardless of the year of occurrence. Pancha and others (in press) compiled these earthquakes from multiple catalogs. Due to improvements in the seismograph network beginning around 1970, all earthquakes with magnitudes of 4.0 and greater that occurred after 1970 were considered detectable regardless of epicenter location, and were added to this compilation. Data for these lower-magnitude earthquakes came from the USGS National Earthquake Information Center and the Berkeley Advanced National Seismic System.

MAGMATICALLY HEATED GEOTHERMAL SYSTEMS

It has long been recognized that high-temperature geothermal activity in the world is closely associated with Quaternary and/or active silicic volcanism (e.g., Smith and Shaw, 1975). In the Great Basin, geothermal systems with suspected shallow-crustal magmatic heat sources are largely restricted to the margins of the Great Basin and are closely associated with Quaternary silicic volcanic rocks (Koenig and McNitt, 1983). Axehart and others (2003) document that these magmatically heated systems have higher fluid concentrations of some trace metals, including As, Li, Cs, and Rb, and higher temperature gradients, as measured from the surface down to their subsurface geothermal reservoirs, than their amagmatic geothermal system counterparts.

The color-scaled probability map discussed above was not designed to predict the occurrence of magmatically heated geothermal systems. Instead, the locations of Quaternary silicic (rhyolite and rhyodacitic) volcanic vents can be used; they were compiled from numerous sources, including the Great Basin Geoscience Database (Raines and others, 1996), and the Geothermal Resources of Utah CD (Blackett and Wakefield, 2002).

DISCUSSION

The ability of the geothermal potential map to correctly predict areas of geothermal potential is dependent on many factors. One limitation is the detail and accuracy of the digital data. The historical earthquake record spans at best 100 years, which is not enough to properly represent earthquake activities on some fault systems that may have recurrence intervals measured in thousands of years. Similarly, the number of tectonic-anchored GPS stations limits the resolution and accuracy of geodesy-based crustal strain estimates. Fault slip-rate estimates are significantly constrained by the small number of detailed trench studies. Additional gravity stations would sharpen the gravity/topographic map. Some types of geological information important for predicting geothermal activity have not been included in the model. For example, some rocks make better reservoir hosts than others (e.g., the Triassic Auld Lang Syne Group and limestones do not make good high-temperature reservoirs (Dick Benoit, personal commun., 2005)). But because host rock lithologies at 1-3 km depths (the assumed range in production depth) are either unknown or are poorly constrained in many areas, host rock compositions were not used.

Another factor potentially limiting the map's predictive potential is the assumption that similar geologic processes control all amagmatic geothermal systems in the Great Basin. This is not likely to be entirely true, because of regional differences in the tectonic setting, style of fracturing, fault-controlled permeability, and the composition of reservoir host rocks. For example, geothermal systems in the Walker Lane may be more closely associated with strike-slip faulting and pull-apart blocks (e.g., the Fish Lake Valley, Stockli and others, 2003) than geothermal systems in the rest of the Great Basin.

In spite of the challenges involved with modeling, the predictive power of the map appears good in many areas, including, for example, Dixie Valley, Surprise Valley, Railroad Valley, Summer Lake, New York Canyon, and the Carlach area. Several of these areas did not have associated geothermal training sites used for modeling, so were not able to influence the results, but good favorability was predicted anyway. Highly favorable geothermal terrain is predicted for portions of the eastern and northeastern Great Basin near and north of Salt Lake City, and in the southwestern Great Basin in and near Saline Valley, Death Valley, and Clayton Valley--some of these areas may warrant a closer look. In any case, the map contains relatively detailed information and in many places provides a thought-provoking interpretation that should challenge current and future explorationists.

GEOTHERMAL INFORMATION

A brief explanation of other information displayed on this map follows:

TEMPERATURE GRADIENT (David Blackwell, SMU):
Uncorrected temperature gradient data from wells in the SMU geothermal database (http://www.smu.edu/geothermal/) are shown, including data from John Sass (USGS). Many of these wells are shallow and the quality of the temperature-estimates vary, but on a regional basis, good temperature anomalies are often defined with these holes.

HEAT FLOW MEASUREMENT (David Blackwell, SMU; John Sass, USGS):
Heat flow calculations from wells in the SMU and USGS geothermal databases are plotted (http://www.smu.edu/geothermal/, http://pubs.usgs.gov/of/2005/1237/). These wells have been selected for their reliability and are better potential indicators of geothermal activity than the temperature gradient holes above.

WELL AND SPRING GEOTHERMOMETER (Geo -Heat Center compiled database):
Estimated maximum geothermal reservoir temperatures for wells and springs in the Geo -Heat Center database (Boyd, 2002, http://geoheat.oit.edu/) are plotted. The color-coded value represents the average of the Na-K-Ca-Mg geothermometers, using the algor ithms proposed by Mariner and others (1983). A database of the geothermometer temperatures shown on the map is available at the web site of the Great Basin Center for Geothermal Energy at http://www.unr.edu/geothermal/geochem.html, (see files GeoHGB_0.xls or GeoHGB_0.snp).

QUATERNARY FAULTS (USGS):
Quaternary faults from the web site (http://gldims.cr.usgs.gov/qfaults/viewer.htm) of the USGS Quaternary Fault and Fold Database are plotted in two d ifferent slip-rate categories. This fault database is a work in progress. Some areas have been more completely mapped than others, and some faults are missing. The USGS plans to periodically update this database with more accurate fault locations and slip -rate data.

ACKNOWLEDGMENTS

Support from the U.S. Department of Energy under instrument number DE-FG07-02ID14311 made this research possible. Lisa Shevenell, current director, and Jane Long, former director of the Great Basin Center for Geothermal Energy, provided key support and encouragement necessary for completion of this project.

REFERENCES

Agterberg, F.P., Bonham-Carter, G.F., Cheng, Q., and Wright, D.F., 1993, Weights of evidence modeling and weighted logistic regression for mineral potential mapping, in Davis, J.C., and Herzfeld, U.C., eds., Computers in Geology, 25 Years of Progress: Oxford University Press, Oxford, UK, p. 13-32.

Arehart, G., Coolbaugh, M.F., and Poulson, S.R., 2003, Evidence for a magmatic source of heat for the Steamboat Springs geothermal system using trace elements and gas geochemistry: Geothermal Resources Council Transactions, v. 27, p. 269-274.

Bennett, R.A., Wernicke, B.P., and Davis, J.L., 1998, Continuous GPS measurements of contemporary deformation across the northern Basin and Range province: Geophysical Research Letters, v. 25, p. 563-566.

Blackett, R.E., and Wakefield, S.I., 2002, Geothermal resources of Utah, a digital atlas of Utah's geothermal resources: Utah Geological Survey Open-File Report 397, CD-ROM.

Blackwell, D.D., and Richards, M., 2004, Geothermal map of North America, AAPG: American Association of Petroleum Geologists, map item number 423, scale 1:6,500,000.

Blewitt, G., Coolbaugh, M.F., Holt, W., Kreemer, C., Davis, J.L., and Bennett, R.A., 2002, Targeting of potential geothermal resources in the Great Basin from regional relationships between geodetic strain and geological structures: Geothermal Resources Council Transactions, v. 26, p. 523-525.

Blewitt, G., Coolbaugh, M., Sawatzky, D., Holt, W., Davis, J., and Bennett, R., 2003, Targeting of potential geothermal resources in the Great Basin from regional to basin-scale relationships between geodetic strain and geological structures: Geothermal Resources Council Transactions, v. 27, p. 3-7.

Bonham-Carter, G.F., 1996, Geographic Information Systems for Geoscientists, Modelling with GIS: Elsevier Science Inc., Tarrytown, NY, 398 p.

Bonham-Carter, G.F., Agterberg, F.P., and Wright, D.F., 1988, Integration of geological datasets for gold exploration in Nova Scotia: Photogrammetric Engineering and Remote Sensing, v. 54, no. 11, p. 1585-1592.

Bowen, R., 1989, Geothermal Resources, 2nd Edition: Elsevier Science Inc., New York, NY, 485 p.

Boyd, T., 2002, Western states geothermal databases CD: Geothermal Resources Council Transactions, v. 26, p. 605-609.

Coolbaugh, M.F., 2003, Fie prediction and detection of geothermal systems at regional and local scales in Nevada using a Geographic Information System, spatial statistics, and thermal infrared imagery [Ph.D. dissertation]: University of Nevada, Reno, 172 p.

Coolbaugh, M.F., Taranik, J.V., Raines, G.L., Shevenell, L.A., Sawatzky, D.L., Minor, T.B., and Bedell, R., 2002, A geothermal GIS for Nevada: defining regional controls and favorable exploration terrains for extensional geothermal systems: Geothermal Resources Council Transactions, v. 26, p. 485-490.

Fenneman, N.M., 1928, Physiographic divisions of the United States: Annals of the Association of American Geographers, v. 18, no. 4, p. 261-353.

Haines, A.J., and Holt, W.E., 1993, A procedure for obtaining the complete horizontal motions within zones of distributed deformation from the inversion of strain-rate data: Journal of Geophysical Research, v. 98, p. 12057-12082.

Hammond, W.C., and Thatcher, W., 2004, Contemporary tectonic deformation of the Basin and Range province, western United States: 10 years of observation with the Global Positioning System: Journal of Geophysical Research, v. 109, p. B08403-B08423.

Holt, W.E., Shen-Tu, B., Haines, J., and Jackson, J., 2000, On the determination of self-consistent strain rate fields within zones of distributed deformation, in Richards, M.A., Gordon, R.G., and van der Hilst, R.D., eds., The History and Dynamics of Global Plate Motions, p. 113-141: American Geophysical Union, Washington, D.C.

Koenig, J.B., and McNitt, J.R., 1983, Controls on the location and intensity of magmatic and non-magmatic geothermal systems in the Basin and Range province: Geothermal Resources Council, Special Report No. 13, p. 93.

Kreemer, C., Haines, A.J., Holt, W.E., Blewitt, G., and Lavallée, D., 2000, On the determination of a global strain rate model: Earth, Planets, and Space, v. 52, p. 765-770.

Machette, M.N., Haller, K.M., Dart, R.L., and Rhea, S.B., 2003, Quaternary fault and fold database of the United States: U.S. Geological Survey Open-File Report 03-417, http://qfaults.cr.usgs.gov/faults/

Mariner, R.H., Presser, T.S., and Evans, W.C., 1983, Geochemistry of active geothermal systems in the northern Basin and Range province: Geothermal Resources Council, Special Report No. 13, p. 95-119.

Pancha, A., Anderson, J.G., and Kreemer, C., in press, Comparison of seismic, geodetic and geological scalar moment rates across the Basin and Range province: Bulletin of the Seismological Society of America.

Prudic, D.E., Harrill, J.R., and Burkey, T.J., 1995, Conceptual evaluation of regional groundwater flow in the carbonate-rock province of the Great Basin, Nevada, Utah, and adjacent states: U.S. Geological Survey Professional Paper 1409-D, 102 p.

Raines, G.L., Sawatzky, D.L., and Connor, K.A., 1996, Great Basin Geoscience Data Base: USGS Digital Data Series DDS-041.

Raines, G.L., Bonham-Carter, G.F., and Kemp, L., 2000, Predictive probabilistic modeling using ArcView GIS: ArcUser, v. 3, no. 2, p. 45-48.

Sass, J.H., Lachenbruch, A.H., Munroe, R.J., Greene, G.W., and Moses, T.H. Jr., 1971, Heat flow in the Western United States: Journal of Geophysical Research, v. 76, p. 6376-6413.

Sass, J.H., Priest, S.S., Blanton, A.J., Sackett, P.C., Welch, S.L., and Walters, M.A., 1999, Geothermal industry temperature profiles from the Great Basin: U.S. Geological Survey Open-File Report 99-425 (http://pubs.usgs.gov/of/1999/of99-425/webmaps/home.html)

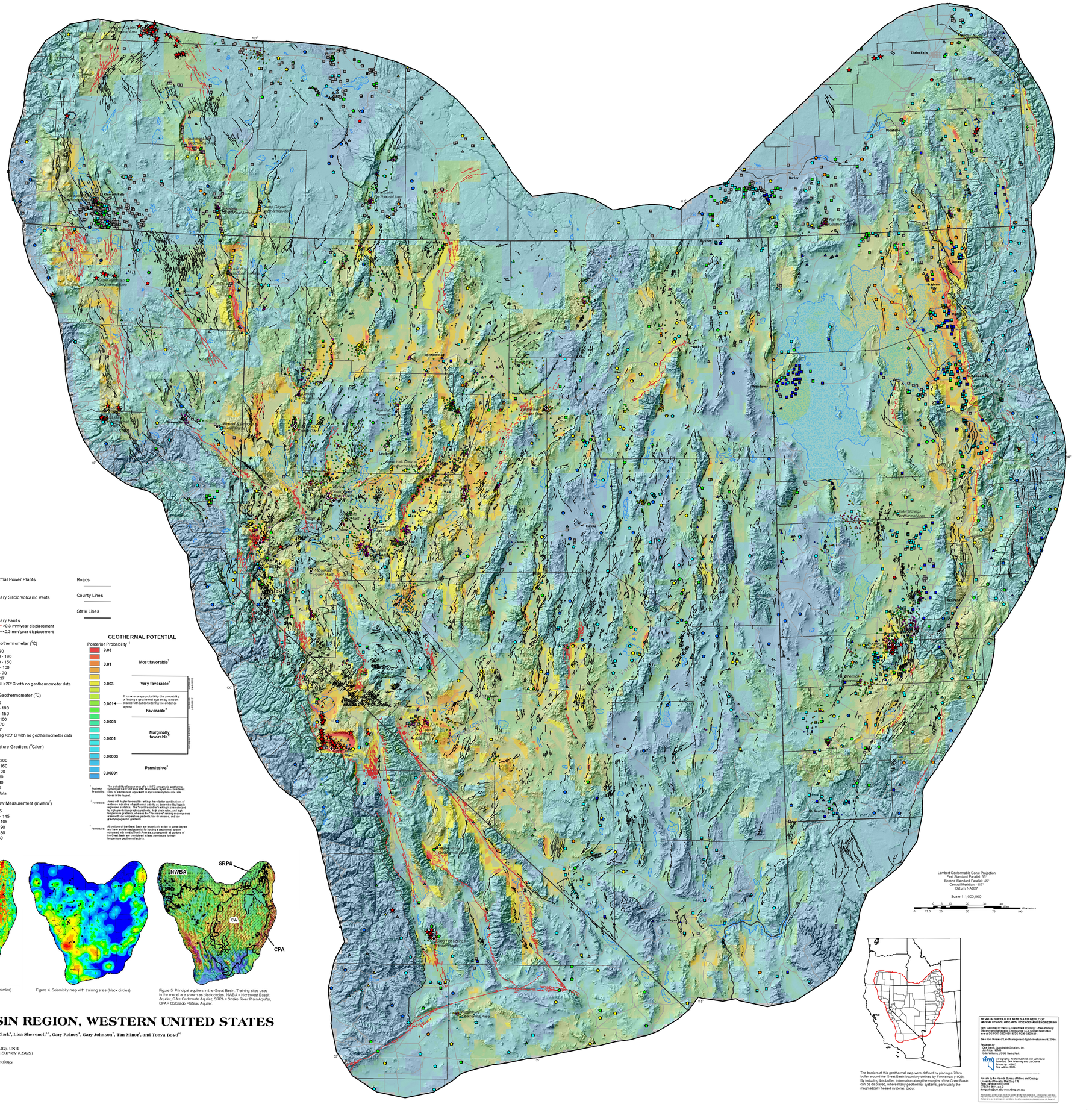
Smith, R.L., and Shaw, H.R., 1975, Igneous-related geothermal systems, in White, D.E. and Williams, D.L., eds., Assessment of Geothermal Resources of the United States--1975: U. S. Geological Survey Circular 726, p. 58-80.

Stockli, D.F., Dumitru, T.A., McWilliams, M.O., and Farley, K.A., 2003, Cenozo ic tectonic evolution of the White Mountains, California and Nevada: Geological Society of America Bulletin, v. 115, no. 7, p. 788-816.

Svarc, J.L., Savage, J.C., Prescott, W.H., and Ramelli, A.R., 2002, Strain accumulation and rotation in western Nevada, 1993-2000: Journal of Geophysical Research, v. 107, p. 2090-2102.

Thelin, G. P., and Pike, R. J., 1991, Landforms of the conterminous United States – A digital shaded-relief portrayal: U.S. Geological Survey, Miscellaneous Investigation Series, Map I-2206, scale 1: 350 000, accompanying booklet, 16 p.

Wisian, K.W., Blackwell, D.D., and Richards, M., 1999, Heat flow in the western United States and extensional geothermal systems: Proceedings 24th Workshop on Geothermal Reservoir Engineering, Stanford, CA, p. 219-226.


Geothermal Power Plants
Quaternary Silicic Volcanic Vents
Quaternary Faults
>0.3 mm/year displacement
<0.3 mm/year displacement
Roads
County Lines
State Lines
GEOTHERMAL POTENTIAL
Posterior Probability [1]
0.03
0.01
0.003
0.0014
0.0003
0.0001
0.00003
0.00001
Most favorable[2]
Very favorable[2]
Favorable[2]
Marginally favorable[2]
Permissive[3]
Increasing Favorability
Prior or average probability (the probability of finding a geothermal system by random chance without considering the evidence layers)
Well Geothermometer (°C)
>190
150 - 190
100 - 150
70 - 100
37 - 70
0 - 37
Well <20°C with no geothermometer data
Spring Geothermometer (°C)
>190
150 - 190
100 - 150
70 - 100
37 - 70
0 - 37
Spring >20°C with no geothermometer data
Temperature Gradient (°C/km)
>200
160 - 200
120 - 160
80 - 120
40 - 80
20 - 40
0 - 20
No Data
Heat Flow Measurement (mW/m2)
>145
105 - 145
90 - 105
80 - 90
60 - 80
0 - 60
Posterior Probability: The probability of occurrence of a >150°C amagmatic geothermal system, based on the input maps. The number of colors displayed (tree of extension is equivalent to approximately two color ramps in the legend.
[2] Favorable: Areas with higher favorability rankings have better combinations of evidence indicative of geothermal activity, as determined by logistic regression statistics. The "Most Favorable" ranking is characterized by high gravity/topographic gradients, high strain rates, and high temperature gradients, whereas the "Favorable" rank encompasses areas with lower temperature gradients, low strain rates, and low gravity/topographic gradients.
[3] Permissive: All portions of the Great Basin are tectonically active to some degree and have an elevated potential for hosting a geothermal system compared with most of North America; consequently, all portions of the Great Basin are considered at least permissive for high-temperature geothermal activity.
Lambert Conformable Conic Projection
First Standard Parallel: 33°
Second Standard Parallel: 45°
Central Meridian: -117°
Datum: NAD27
Scale 1:1,000,000
0 12.5 25 50 75 100 Kilometers
0 5 10 20 30 40 Miles
Las Vegas
Reno
Salt Lake City
Boise
Idaho Falls
Pocatello
Elko
Ely
Winnemucca
Battle Mountain
Lovelock
Fallon
Carson City
Tonopah
Beatty
Hawthorne
Fernley
Wendover
Tooele
Provo
Richfield
Cedar City
Delta
Fillmore
Milford
Panaca
Caliente
Pioche
Ely
Wells
Jackpot
Owyhee
Winnemucca
Lovelock
Fallon
Fernley
Hawthorne
Tonopah
Beatty
Caliente
Pioche
Delta
Fillmore
Milford
Richfield
Cedar City
Provo
Tooele
Wendover
Elko
Wells
Jackpot
Owyhee
Idaho Falls
Pocatello
Boise
Salt Lake City
Las Vegas
Reno
Carson City
Battle Mountain
Lovelock
Fallon
Fernley
Hawthorne
Tonopah
Beatty
Caliente
Pioche
Ely
Wells
Jackpot
Owyhee
Winnemucca
Elko
Wendover
Tooele
Provo
Richfield
Cedar City
Delta
Fillmore
Milford
Panaca